AIP | Applied Physics Letters

# Hierarchical elasticity of bimesogenic liquid crystals with twist-bend nematic phase

Chang-Jun Yun, M. R. Vengatesan, Jagdish K. Vij, and Jang-Kun Song

Citation: Applied Physics Letters **106**, 173102 (2015); doi: 10.1063/1.4919065
View online: http://dx.doi.org/10.1063/1.4919065
View Table of Contents: http://scitation.aip.org/content/aip/journal/apl/106/17?ver=pdfcov
Published by the AIP Publishing



# Hierarchical elasticity of bimesogenic liquid crystals with twist-bend nematic phase

Chang-Jun Yun,[1,2] M. R. Vengatesan,[1,3] Jagdish K. Vij,[4] and Jang-Kun Song[1,a)]
[1]School of Electronic and Electrical Engineering, Sungkyunkwan University, Suwon, 400-746, Korea
[2]Advanced Technology Center, Merck Advanced Technologies Ltd., Pyeongtaek 451-822, Korea
[3]Department of Chemical Engineering, The Petroleum Institute, Abu Dhabi, 2533, United Arab Emirates
[4]Department of Electronic and Electrical Engineering, Trinity College, University of Dublin, Dublin 2, Ireland

(Received 22 February 2015; accepted 14 April 2015; published online 27 April 2015)

In 2001, Dozov predicted that twist-bend nematic phase can be spontaneously formed when $K_{33} < 0$ and $K_{11}/K_{22} > 2$, and this phase has recently been discovered in bimesogens. To verify Dozov's hypothesis, we have measured precisely the temperature dependence of the elastic constants of CB7CB in the entire temperature range of nematic phase and in twist-bend nematic phase close to the transition temperature by combing the Fréedericksz threshold methods for a twist nematic and an in-plane switching cells. Anomalous changes in $K_{22}$ and $K_{33}$ are observed across the phase transition. The elasticity estimated via extrapolation of the data in the high temperature region of the nematic phase seems to fully satisfy Dozov's hypothesis although the elasticity data in the vicinity of the phase transition exhibit opposite trends. This can be explained by the general nature of a hierarchical system where the macroscopic elasticity is governed mostly by the distortion of a higher level structure. © *2015 AIP Publishing LLC*. [http://dx.doi.org/10.1063/1.4919065]

In the past few years, bimesogenic liquid crystals have been studied for their remarkable physical properties and fascinating features, such as their anomalous elastic behavior[1,2] and large flexoelectric coefficients,[3,4] which have potential applicability in nano-technology[5] and energy harvesting.[6] In particular, some bimesogenic liquid crystals with an odd number of methylene flexible units or a rigid bent-core mesogen showed an additional nematic phase at temperatures below the conventional nematic phase ($N_u$).[7,8] Recently, this phase has been identified as the twist-bend nematic phase ($N_{tb}$),[9] where the director forms periodic twisted and bent deformations with a nano-scale pitch (8–9 nm).[10] In planar cells, the $N_{tb}$ phase also exhibited spontaneous periodic stripe patterns in micrometer-scale.[7,11] Although the latter is reminiscent of the smectic phase, X-ray scattering patterns and nuclear magnetic resonance spectroscopy indicated that the $N_{tb}$ phase is nematic-like rather than of the lamellar type.[2,12–14]

The twist-bend nematic phase was predicted by Meyer in 1973 in chiral molecules,[15] and Dozov predicted spontaneous symmetry-breaking in an achiral banana-shaped mesogen. Such a structure could be formed through either splay-bend deformations or a conical twist-bend helix if the bend elastic constant ($K_{33}$) becomes negative.[16] Dozov determined that the twist-bend phase is much more stable than the splay-bend when the twist elastic constant ($K_{22}$) is less than half of the splay elastic constant ($K_{11}$).

Balachandran *et al*. reported that $K_{11}$ of a typical bimesogen, CB11CB, increased with the decrease in temperature while $K_{33}$ decreased or remained almost temperature-independent in $N_u$ phase.[1] After extrapolation of the experimental results, there was no indication of $K_{33}$ turning negative in the $N_{tb}$ phase. Adlem *et al*. reconfirmed these tendencies for a mixture of dimers. In their results, $K_{33}$ tended to zero as the temperature decreased close to the $N_u$-$N_{tb}$ phase transition temperature ($T_{Nu\text{-}Ntb}$),[2] but $K_{33}$ could not be extrapolated to a negative value through temperature reduction. Important questions still remain to be answered, such as how the elastic constants behave closer to $T_{Nu\text{-}Ntb}$, especially below $T_{Nu\text{-}Ntb}$.[1]

Herein, we focus on the study of the elastic constants from the ordinary nematic phase to the temperature range just below the $N_u$-$N_{tb}$ phase transition via precise temperature control. We found a diverging trend of $K_{33}$ just below the $N_u$-$N_{tb}$ phase transition, and observed anomalous behavior of $K_{11}$. These observations do not agree with the predictions of Dozov, and could be explained by the hierarchical structural nature of the $N_{tb}$ phase. The elasticity close to the $N_u$-$N_{tb}$ transition is governed by the macroscopic distortions of the high level structure rather than caused by the conventional elastic distortion.

The material used herein is 1″,7″-bis(4-cyanobiphenyl-4′-yl) heptanes (CB7CB) that was synthesized in our laboratory.[17] A differential scanning calorimetric (DSC) analysis revealed clear $N_u$-$N_{tb}$ transition at 99.0 °C on heating and at 98.6 °C on cooling.[17]

As shown in Fig. 1, polarized optical microscopy (POM) was used to investigate thin and thick planar cells as well as a non-surface-treated cell. The temperature was controlled precisely using a hot stage (TMS94 and LTS350, Linkam, USA), and in the POM observations, $T_{Nu\text{-}Ntb}$ was determined to be 99.6 °C, at which the nematic thermal fluctuation started to disappear[7] and the opposite handedness helical domains started to appear (Figs. 1(a-ii) and 1(c-ii)).[11,18] In a 3.2-$\mu$m-thick planar cell, micro-scale stripe patterns grew along the rubbing direction (Fig. 1(a-iii)) and gradually spread across the entire cell area on cooling (Fig. 1(a-iv)).[1,7] In a non-surface-treated 3.8-$\mu$m-thick cell, focal-conic defect textures appeared at 99.3 °C (Fig. 1(b-iii)) and fine stripes filled each

a)E-mail: jk.song@skku.edu

 

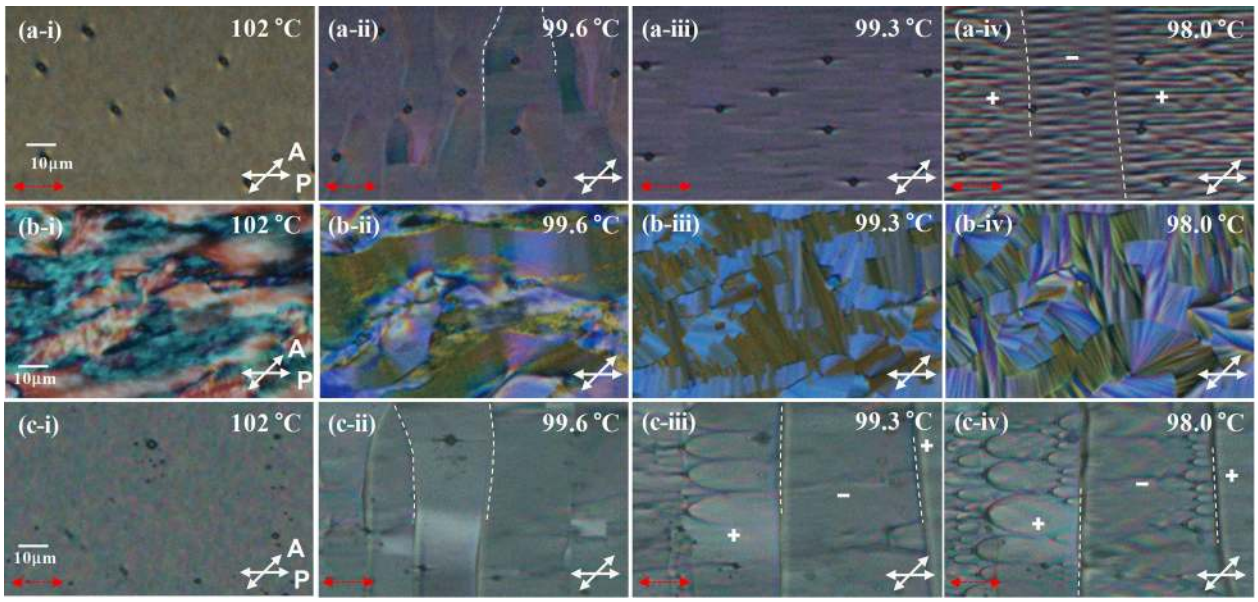


FIG. 1. POM images of CB7CB cells with decreasing temperature for a thin planar cell (3.2 $\mu$m thickness) ((a-i)–(a-iv)), for a thin non-rubbed cell (3.8 $\mu$m) ((b-i)–(b-iv)), and for a thick planar cell (25 $\mu$m) ((c-i)–(c-iv)). (a-i), (b-i), and (c-i) are for $N_u$ phase. At 99.6 °C (= $T_{Ntb\text{-}Nu}$), nematic thermal fluctuation started to disappear and opposite handedness helical domains started to grow (the dotted domain boundaries in (a-ii) and (c-ii)).[7,11,18] With further cooling, stripe textures with 3.08 $\mu$m half-pitch were developed ((a-iii) and (a-iv)). In non-rubbed cell, focal conic textures appeared ((b-ii) and (b-iii)) and stripe patterns were embedded within the focal-conic domains with further cooling (b-iv). Parabolic textures were dominantly observed below $T_{Ntb\text{-}Nu}$ in a thick cell ((c-ii), (c-iii), and (c-iv)). The red arrow denotes the rubbing direction. The polarizer and analyzer (the white solid arrows) were arranged to make 45° with respect to each other to give clear images.

focal-conic domain after further cooling (Fig. 1(b-iv)). In a 25-$\mu$m-thick rubbed planar cell, uniform nematic ordering in the $N_u$ phase (Fig. 1(c-i)) turned into parabolic defect textures below $T_{Nu\text{-}Ntb}$ (Fig. 1(c-iii)), and the textures became denser with further cooling (Fig. 1(c-iv)). Previously, both parabolic and focal-conic defect textures, commonly found in smectic and cholesteric nematic phases, were observed in odd-methylene linked dimers.[12,14]

Interestingly, upon cooling of the cells, the fanlike focal-conic defect textures first appear at $T_{Nu\text{-}Ntb}$ and then the rope-like stripe patterns appeared when cooled further. Note that the fanlike defects in smectic and cholesteric nematic phases are created by the deformation of a long-range higher level hierarchical structure rather than by a low-level intermolecular elastic deformation.[19] As shown in Fig. 1, the focal-conic textures were observed just before the appearance of the unique micro-scale stripe patterns on cooling (Fig. 1(a-iv)), indicating that these patterns are the result of a higher structural deformation like as in smectic and cholesteric phases.

Using a 25-$\mu$m-thick planar cell, dielectric anisotropy ($\varepsilon_{||} - \varepsilon_{\perp}$) was measured at 1 kHz. The $\varepsilon_{\perp}$ value was obtained without applying a bias voltage, while $\varepsilon_{||}$ was obtained from the capacitance measured at a high bias voltage to induce a vertical alignment. The capacitance was not fully saturated up to 20 V, although its slope decreased with increasing voltage. It was empirically found that the capacitance linearly increases as the reciprocal value of the applied voltage decreases, and we could approximate the saturated capacitance using the relationship (see Ref. 17 for details). As shown in Fig. 2, the dielectric anisotropy of CB7CB shows positive values and decreases upon cooling using the same hot-stage used for POM observation. For conventional calamitic liquid crystals, $\varepsilon_{||}$ increases when cooled, but for CB7CB, both $\varepsilon_{||}$ and $\varepsilon_{\perp}$ decrease with decreasing temperatures, as already reported.[1,12] Cestari *et al*. explained that this phenomenon can be modeled by changes in the conformational distribution of the molecules, which decrease the macroscopic orientational order parameter with decreasing temperatures. This result indicates that the molecular ordering of CB7CB differs from the conventional nematic ordering, even in the $N_u$ phase.

$K_{11}$ and $K_{33}$ were determined using the standard Fréedericksz threshold method. $K_{11}$ was calculated from the equation $K_{11} = V_{th}{}^2 \varepsilon_0 \Delta\varepsilon/\pi^2$. In order to calculate $K_{33}$, the voltage-capacitance curve was fitted to the following expression:[20]

$$\frac{C}{C_0} = \frac{2}{\pi}\sqrt{1+\gamma\sin^2\theta_m}\frac{V_{th}}{V}\int_0^{\theta_m}\sqrt{\frac{(1+\gamma\sin^2\theta)(1+K\sin^2\theta)}{\sin^2\theta_m - \sin^2\theta}}d\theta, \tag{1}$$

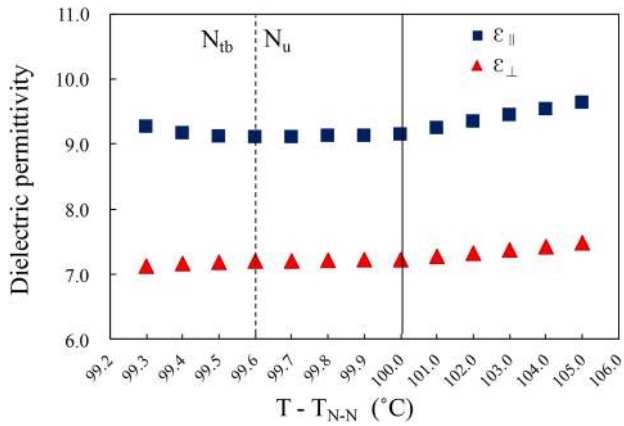


FIG. 2. Temperature dependencies of the parallel ($\varepsilon_{||}$) and perpendicular ($\varepsilon_{\perp}$) components of the dielectric permittivity. The abscissa exhibits different temperature scales on either side of the solid vertical line.

in which $K=(K_{33}-K_{11})/K_{11}$, $\gamma=(\varepsilon_{||}-\varepsilon_{\perp})/\varepsilon_{\perp}$, and $\theta_m$ is the tilt angle at the center of the liquid crystal layer.

Several approaches have been employed to measure $K_{22}$. These are the Fréedericksz threshold methods using a twisted nematic (TN) cell, an in-plane switching (IPS) cell, a wedge cell, a $\pi$-cell, or a light scattering method.[21] However, in all these methods, the measured value of $K_{22}$ is usually less accurate than those of $K_{11}$ and $K_{33}$.

First, we measure $K_{22}$ using a TN cell. $K_{22}$ was calculated by using the already measured $K_{11}$, $K_{33}$, and $V_{th}$ (threshold voltage) values:

$$V_{th}^{TN}=\pi\left(\frac{K_{TN}}{\varepsilon_0\Delta\varepsilon}\right)^{1/2},\quad \text{where } K_{TN}=\frac{(4K_{11}+K_{33}-2K_{22})}{4}. \tag{2}$$

Equation (2) shows that $K_{22}$ depends on $K_{11}$ and $K_{33}$. Through $K_{TN}$, the errors in $K_{11}$ and $K_{33}$ are directly reflected in the value of $K_{22}$. In particular, in the vicinity of $T_{Nu\text{-}Ntb}$, large variations in $K_{11}$ and $K_{33}$ were observed, with inevitable errors in $K_{22}$. As a result, the measured values of $K_{22}$ near the phase transition were somewhat inaccurate and elusive.[17]

To mitigate errors in the measurement of $K_{22}$ near the phase transition, we used a method that employs an IPS cell.[22] In this method, the twist elastic constant is related to the threshold voltage $V_{th}^{IPS}$ by

$$V_{th}^{IPS}=\frac{\pi l}{d}\left(\frac{K_{22}}{\varepsilon_0\Delta\varepsilon}\right)^{1/2}. \tag{3}$$

Herein, $l$ is the electrode distance and $d$ is the cell thickness. Using Eq. (3), it is possible to find $K_{22}$ independently of the other two elastic constants. However, it is difficult to find the accurate value of $K_{22}$ with this method too, since the voltage-to-transmittance curve in an IPS cell slowly changes near the threshold voltage, generating errors in the determination of $V_{th}^{IPS}$. Moreover, the electric field within an IPS cell is not uniform, causing an error; since Eq. (3) was derived using a uniform field-approximation. However, the temperature dependence of $K_{22}$ is accurate enough. Hence, by combining the two methods, we can obtain more reliable values of $K_{22}$ in the vicinity of $T_{Nu\text{-}Ntb}$.[17] $K_{22}$ was determined using the data obtained from a IPS cell after tuning the absolute values based on the data obtained from TN cell (see Ref. 17). The cell thicknesses of the TN and IPS cells were 3.2 $\mu$m and 3.27 $\mu$m, respectively.

It was not possible to measure either the dielectric anisotropy or the elastic constants in the $N_{tb}$ phase below 99.3 °C because of the high viscosity. We measured the elastic constants from 105 °C to 100 °C with 1 °C intervals, and from 100 °C to 99.3 °C with 0.1 °C intervals (Fig. 3(a)). In $N_u$ phase, $K_{11}$ and $K_{22}$ increased almost linearly with decreasing temperature, and $K_{33}$ decreased linearly. In conventional nematics, $K_{33}$ is usually larger than $K_{11}$,[23] but $K_{33}$ for CB7CB was significantly lower than $K_{11}$. Below the $N_u$-$N_{tb}$ phase transition, dramatic changes in the elastic properties are found. Interestingly, the bend elastic constant increased anomalously from 0.3 pN at $T_{Nu\text{-}Ntb}$ to 47.4 pN at $T_{Nu\text{-}Ntb}$ −0.3 °C. Adlem *et al.* also found a slight increase of $K_{33}$ in the pretransitional region in a different system, but the increase was not dramatic as much as observed here.[2]

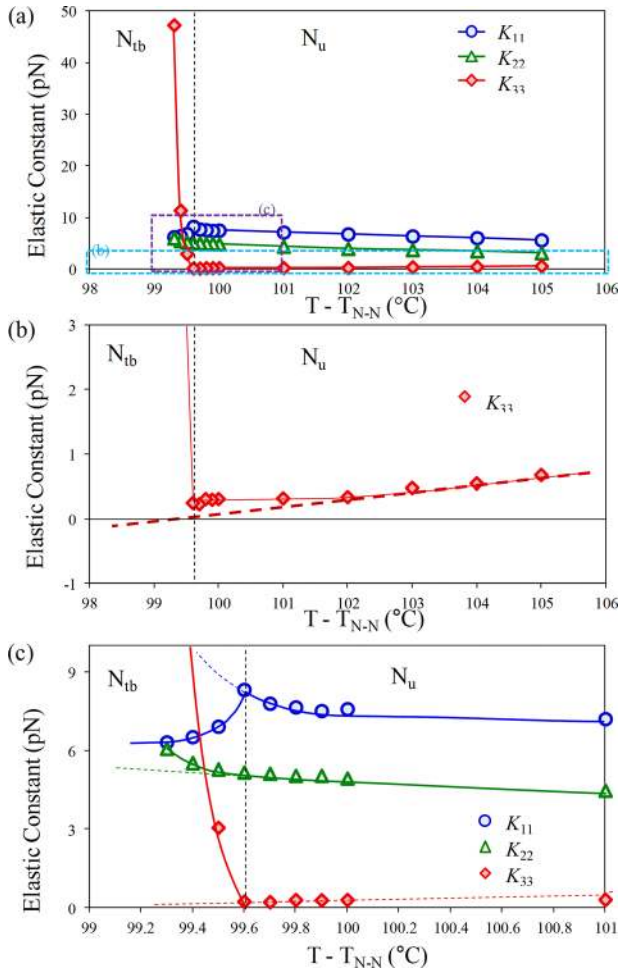


FIG. 3. (a) $K_{11}$, $K_{22}$, and $K_{33}$ elastic constants as a function of the reduced temperature at 1 kHz. (b) Expanded vertical scale and extrapolation for $K_{33}$. (c) Expanded horizontal scale and the anomalous behaviors of the elastic constants below $T_{Ntb\text{-}Nu}$.

These elastic behaviors are reminiscent of those in the vicinity of nematic to smectic-A or smectic-C phase transition in bent-core systems.[23,24] The abnormal tendency in $K_{33}$ was explained by smectic short-range fluctuations as the temperature decreased.[2,24] The focal-conic and parabolic defect textures were observed in both the smectic and $N_{tb}$ phases.[12,14,25]

To make a detailed investigation of the elastic constants in the $N_{tb}$ phase, expanded scales of the obtained curves are shown in Figs. 3(b) and 3(c). In Fig. 3(b), where the vertical scale is expanded for $K_{33}$, the linear extrapolation extending from the high-temperature $K_{33}$ values crosses zero at $T_{Nu\text{-}Ntb}$, as indicated by the dashed line. However, this linear extrapolation slightly deviates from the experimental data as the temperature decreases below 102 °C, and moreover, $K_{33}$ abruptly increases instead of decreasing further down for temperatures below $T_{Nu\text{-}Ntb}$. This shows that a negative $K_{33}$ in the $N_{tb}$ phase is not a real possibility. In Fig. 3(c), the horizontal temperature axis is expanded to show the elastic behavior near $T_{Nu\text{-}Ntb}$. Interestingly, at $T_{Nu\text{-}Ntb}$, $K_{11}$ also abruptly changes its increasing trend into a decreasing one as the temperature decreases. Thus, unexpected changes in $K_{11}$ and $K_{33}$ have been observed when the temperature crosses $T_{Nu\text{-}Ntb}$. Finally, for $K_{22}$, a rather constant slope is observed, although the slope slightly changes below $T_{Nu\text{-}Ntb}$.

The ratio of $K_{11}/K_{22}$ was more or less constant with a value of approximately 1.4 in the $N_u$ phase, which is much lower than 2. Below $T_{Nu\text{-}Ntb}$, $K_{11}/K_{22}$ decreases further, thereby approaching 1. This does not agree with the predictions of Dozov, stating that the twist-band nematic phase is stable when $K_{11}/K_{22} > 2$. However, a close look for $K_{11}$ and $K_{22}$ in the $N_u$ region with exception of the data in the $N_{tb}$ phase region reveals slightly different trends from those in the $N_{tb}$ phase. While $K_{22}$ increases linearly with decreasing temperature, $K_{11}$ increases exponentially near $T_{Nu\text{-}Ntb}$ with decreasing temperature (see the dashed extrapolation lines in Fig. 3(c)). The hypothetical extrapolation exhibits a sharp increase of $K_{11}/K_{22}$, which approximately approaches 2 at 0.5–1 °C below $T_{Nu\text{-}Ntb}$.

Interestingly, Dozov's predictions for the twist-bend deformation are fully satisfied if only extrapolations of the elastic constants in the high-temperature range of the $N_u$ phase are taken into consideration, as shown in Figs. 3(b) and 3(c). However, the actual experimental data below $T_{Nu\text{-}Ntb}$ give a totally different picture. Application of an external force to the $N_u$ phase causes a distortion of the molecular level director profile, in which the elastic free energy can be expressed by the sum of three principal distortion energy formulae. However, the $N_{tb}$ phase exhibits spontaneous twist-bend deformations (Fig. 4(a)), which is unlikely to be unwound by applying weak electric fields, as confirmed by electro-optical experiments. Hence, the molecular scale director profile in the nano-scale twist-bend structure is hardly deformed, and instead, the macroscopic long-range structure will be deformed when a significant field is applied. Therefore, the macroscopic elasticity measurement does not reflect the elasticity at the molecular level, but it is related to the elasticity of the higher level hierarchical structure.

The overall temperature-elasticity diagram shows that the extrapolated elasticity estimated from the data at high temperature $N_u$ phase reflects the elasticity of molecular level ordering, but the experimental data at the $N_{tb}$ phase result from the elasticity of a higher-level structure. In the top illustration of Fig. 4(a), small arrows denote the molecular level director (**n**) and the large thick arrows denote the direction of the twist-bend helix, which can be regarded as the higher level director (**N**). The derivation of Dozov's hypothesis was based on the distortion of **n** field by assuming a conventional nematic ordering as the ground state. However, once the twist-bend deformation appears either locally or globally, the uniform nematic ordering becomes one of highly unstable states, resulting in a shift of the ground state. The hierarchical $N_{tb}$ phase should be described based on the deformation of the higher hierarchical structure, which may be achievable by introducing **N** field in the elastic free energy formulae and by assuming the internal twist-bend helix almost invariant. Here, the corresponding effective elastic constants have nothing to do with the molecular level elasticity. The bottom illustration in Fig. 4(a) shows the ground state in the $N_{tb}$ phase, in which **N** field has uniform alignment without distortion while **n** field is highly coiled. Note that the helical equi-phase planes are perpendicular to **N**.

The abrupt changes in $K_{33}$ and $K_{11}$ below $T_{Nu\text{-}Ntb}$ in Fig. 3 suggest that the bend deformation of **N** field is quite elusive but its splay deformation becomes easier. The bending of **N** field accompanies a shrinkage and expansion of the helical pitch ($h$) in order to have the equi-phase plane perpendicular to **N** field (Fig. 4(b-i)). The variation of $h$ requires too large energy and is not feasible. An alternative bend deformation can be conceived by tilting the equi-phase plane from the normal direction of **N** (Fig. 4(b-ii)), in which the effective periodic pitch will reduce to $h{\cdot}\cos\theta$ (here, $\theta$ is the tilting angle of the equi-phase plane) and a strong twist deformation of molecular level director appears along the normal to **N**. Either case of the bend structures costs a large energy, qualitatively explaining the abrupt increase in $K_{33}$. On the other hand, the splay deformation does not accompany such a distortion in the helical pitch (Fig. 4(c)). These features may be able to explain the spontaneous formation of various micro-scale stripe patterns in the $N_{tb}$ phase. Panov *et al.* suggested that the micro-scale stripe textures can be explained by a periodic splay deformation,[7] which qualitatively accords well with our conclusion. Explicit theoretical description may need to consider the effect of equi-phase planes and it remains as a future work.

When the conventional nematic ordering is taken as the datum point as Dozov did in his theory, the twist-bend deformation can be obtained only if $K_{33} < 0$ and $K_{11} > 2K_{22}$. However, in the $N_{tb}$ phase regime, one cannot experimentally

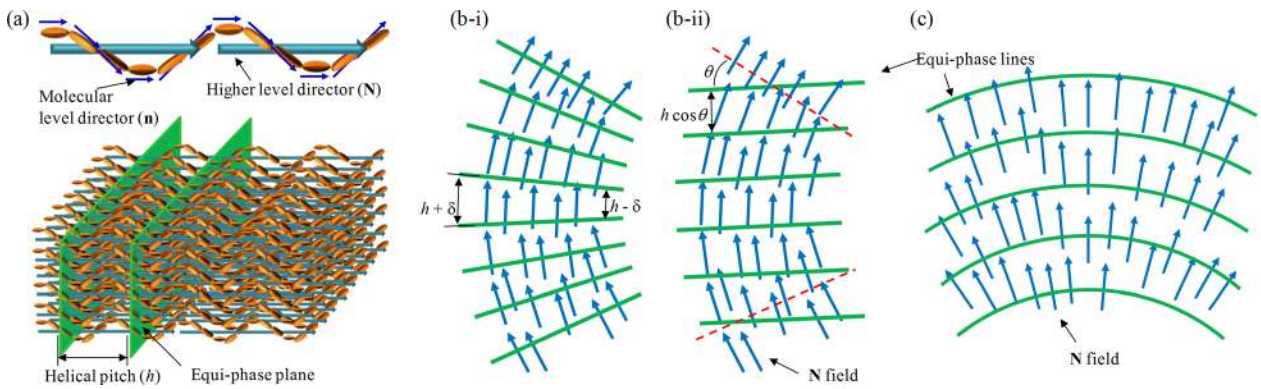


FIG. 4. (a) Molecular arrangement in $N_{tb}$ phase, and the corresponding molecular level director (**n**) and the higher level director (**N**). In uniform $N_{tb}$ phase, **N** field is uniform and equi-phase planes are perpendicular to **N**. (b-i) Bend deformation of N fields accompanies with the helical expansion and shrinkage, or (b-ii) it causes the equi-phase plane to tilt from the normal state, giving a rise to an increase of elastic deformation along the red dashed line. (c) Splay deformation of N fields does not cause a change in the helical pitch.

obtain such a result not because of experimental difficulties but because of the hierarchical nature of the twist-bend nematic phase. Thus, we can conclude that Dozov's hypothesis is only valid as a theoretical description based on the conventional criterion of nematic ordering. We believe that these findings will expand our understanding of the $N_{tb}$ phase which will aid us in devising applications for bimesogenic materials. Some of the possibilities are nano- and micro-templates and imprinting by manipulating the nano- and micro-periodic structure of $N_{tb}$ phase. These can be used in photonic-crystal devices, and micro-mechanical energy harvesting devices that collect the electric energy from the mechanical-deformation-induced polarization of $N_{tb}$ phase with high flexoelectricity. This is highly desired in portable and wearable devices.[3,5,6]

This work was supported by the National Research Foundation of Korea (NRF) Grant funded by MSIP (No. 2014R1A2A1A11054392), and partially by the IT R&D program of MKE/KEIT (No.10041596). J.K.V.'s work was partly supported by Science Foundation of Ireland (SFI) (13/US/I2866), and by US-Ireland R&D Partnership Program jointly administrated with the United States NSF (NSF-DMR-1410649).

[1]R. Balachandran, V. P. Panov, J. K. Vij, A. Kocot, M. G. Tamba, A. Kohlmeier, and G. H. Mehl, Liq. Cryst. **40**(5), 681 (2013).
[2]K. Adlem, M. Čopič, G. R. Luckhurst, A. Mertelj, O. Parri, R. M. Richardson, B. D. Snow, B. A. Timimi, R. P. Tuffin, and D. Wilkes, Phys. Rev. E **88**, 022503 (2013).
[3]R. Balachandran, V. P. Panov, Y. P. Panarin, J. K. Vij, M. G. Tamba, G. H. Mehl, and J. K. Song, J. Mater. Chem. C **2**, 8179 (2014).
[4]S. Morris, M. Clarke, A. Blatch, and H. Coles, Phys. Rev. E **75**, 041701 (2007).
[5]U. Tkalec, M. Ravnik, S. Copar, S. Zumer, and I. Musevic, Science **333**(6038), 62 (2011).
[6]J. Harden, M. Chambers, R. Verduzco, P. Luchette, J. T. Gleeson, S. Sprunt, and A. Jákli, Appl. Phys. Lett. **96**(10), 102907 (2010).
[7]V. P. Panov, M. Nagaraj, J. K. Vij, Y. P. Panarin, A. Kohlmeier, M. G. Tamba, R. A. Lewis, and G. H. Mehl, Phys. Rev. Lett. **105**, 167801 (2010).
[8]D. Chen, M. Nakata, R. Shao, M. R. Tuchband, M. Shuai, U. Baumeister, W. Weissflog, D. M. Walba, M. A. Glaser, J. E. Maclennan *et al.*, Phys. Rev. E **89**, 022506 (2014).
[9]C. Meyer, G. R. Luckhurst, and I. Dozov, Phys. Rev. Lett. **111**, 067801 (2013).
[10]V. Borshch, Y. K. Kim, J. Xiang, M. Gao, A. Jakli, V. P. Panov, J. K. Vij, C. T. Imrie, M. G. Tamba, G. H. Mehl *et al.*, Nat. Commun. **4**, 2635 (2013); D. Chen, J. H. Porada, J. B. Hooper, A. Klittnick, Y. Shen, M. R. Tuchband, E. Korblova, D. Bedrov, D. M. Walba, M. A. Glaser *et al.*, Proc. Natl. Acad. Sci. USA **110**(40), 15931 (2013).
[11]V. P. Panov, R. Balachandran, J. K. Vij, M. G. Tamba, A. Kohlmeier, and G. H. Mehl, Appl. Phys. Lett. **101**(23), 234106 (2012).
[12]M. Cestari, S. Diez-Berart, D. A. Dunmur, A. Ferrarini, M. R. de la Fuente, D. J. B. Jackson, D. O. Lopez, G. R. Luckhurst, M. A. Perez-Jubindo, R. M. Richardson *et al.*, Phys. Rev. E **84**, 031704 (2011).
[13]C. Greco, G. R. Luckhurst, and A. Ferrarini, Phys. Chem. Chem. Phys. **15**(36), 14961 (2013); V. P. Panov, R. Balachandran, M. Nagaraj, J. K. Vij, M. G. Tamba, A. Kohlmeier, and G. H. Mehl, Appl. Phys. Lett. **99**(26), 261903 (2011).
[14]R. J. Mandle, E. J. Davis, C. T. Archbold, S. J. Cowling, and J. W. Goodby, J. Mater. Chem. C **2**(3), 556 (2014).
[15]R. B. Meyer, "Structural problems in liquid crystal physics," in *Molecular Fluids* (Gordon and Breach, Les Houches, 1976), pp. 247–253.
[16]I. Dozov, Euro Phys. Lett. **56**(2), 247 (2001).
[17]See Supplementary material at http://dx.doi.org/10.1063/1.4919065 for the additional experimental information of mateiral, DSC analysis, dielectric analysis, and $K_{22}$ measurement.
[18]C. Meyer, G. R. Luckhurst, and I. Dozov, J. Mater. Chem. C **3**, 318 (2015).
[19]D. Demus, J. W. Goodby, G. W. Gray, and H.-W. Spiess, in *Handbook of Liquid Crystals* (Wiley-VCH, Weinheim, Germany, 1998), Vol. 1.
[20]H. J. Deuling, Mol. Cryst. Liq. Cryst. **19**, 123 (1972).
[21]E. P. Raynes, C. V. Brown, and J. F. Strömer, App. Phys. Lett. **82**(1), 13 (2003); P. D. Brimicombe, C. Kischka, S. J. Elston, and E. P. Raynes, J. App. Phys. **101**(4), 043108 (2007).
[22]K. Ikeda, H. Okada, H. Onnagawa, and S. Sugimori, J. App. Phys. **86**(10), 5413 (1999).
[23]B. Kundu, R. Pratibha, and N. Madhusudana, Phys. Rev. Lett. **99**, 247802 (2007).
[24]P. Sathyanarayana, B. K. Sadashiva, and S. Dhara, Soft Matter **7**(18), 8556 (2011); P. Sathyanarayana, M. Mathew, Q. Li, V. S. S. Sastry, B. Kundu, K. V. Le, H. Takezoe, and S. Dhara, Phys. Rev. E **81**, 010702(R) (2010).
[25]S. Kaur, L. Tian, H. Liu, C. Greco, A. Ferrarini, J. Seltmann, M. Lehmann, and H. F. Gleeson, J. Mater. Chem. C **1**(13), 2416 (2013).